

Separation of $e^+e^- \rightarrow e^+e^-$ and $e^+e^- \rightarrow \pi^+\pi^-$ events using SND detector calorimeter.

M.N. Achasov^{a,b}, K.I. Beloborodov^{a,b}, A. S. Kupich^{a,b*}

*^aBudker Institute of Nuclear Physics, Siberian Branch of the Russian Academy of Science,
11 Lavrentyev, Novosibirsk 630090, Russia*

*^bNovosibirsk State University,
Novosibirsk 630090, Russia*

E-mail: kupich@inp.nsk.su

ABSTRACT: The technique of discrimination of the $e^+e^- \rightarrow e^+e^-$ and $e^+e^- \rightarrow \pi^+\pi^-$ events in energy range $0.5 < \sqrt{s} < 1$ GeV by energy deposition in the calorimeter of SND detector was developed by applying machine learning method. Identification efficiency for $e^+e^- \rightarrow e^+e^-$ and $e^+e^- \rightarrow \pi^+\pi^-$ events in the range from 99.3 to 99.8 % has been achieved.

KEYWORDS: e^+e^- annihilation, particle identification, calorimeter.

*Corresponding author.

Contents

1. Introduction	1
2. The SND calorimeter	2
3. Separation parameter	3
4. Identification efficiency	5
5. Conclusion	8

1. Introduction

The spherical neutral detector SND [1] (Fig.1) is a general purpose nonmagnetic detector operating at VEPP-2000 e^+e^- collider in the center-of-mass energy range from 0.2 to 2.0 GeV [2]. Experimental studies include measurement of the cross sections of the e^+e^- annihilation to hadrons. These measurements are largely motivated by the need of high-precision calculation of the hadronic contribution to the anomalous magnetic moment of the muon $(g-2)/2$ [3]. In particular, the $e^+e^- \rightarrow \pi^+\pi^-$ cross section at the energy region below 1 GeV gives the dominant contribution to this value and should be measured with accuracy higher than 1% [4].

The cross section of the $e^+e^- \rightarrow \pi^+\pi^-$ process is measured in the following way. The collinear events $e^+e^- \rightarrow e^+e^-, \pi^+\pi^-, \mu^+\mu^-$ are selected. The selected events are divided into two classes: e^+e^- and $\pi^+\pi^-, \mu^+\mu^-$. The events of the $e^+e^- \rightarrow \mu^+\mu^-$ process are subtracted according to the theoretical cross section, integrated luminosity and detection efficiency. The cross section of the $e^+e^- \rightarrow \pi^+\pi^-$ process is obtained as follows [5].

$$\sigma_{\pi\pi} = \frac{N_{\pi\pi}}{N_{ee}} \frac{\varepsilon_{ee}}{\varepsilon_{\pi\pi}} \frac{\sigma_{ee}}{1 + \delta_r} \quad (1.1)$$

Here $1 + \delta_r$ is radiative correction, $N_{\pi\pi,ee}$ and $\varepsilon_{\pi\pi,ee}$ are the events numbers and detection efficiencies of the processes $e^+e^- \rightarrow \pi^+\pi^-$ and e^+e^- respectively, σ_{ee} is cross section of the $e^+e^- \rightarrow e^+e^-$ process.

The $e^+e^- \rightarrow e^+e^-, \mu^+\mu^-$ and $\pi^+\pi^-$ events differ by the energy deposition in the calorimeter. In $e^+e^- \rightarrow e^+e^-$ events the electrons produce the electromagnetic shower with the most probable energy losses of about 92% of the initial particle energy. Muons lose their energy by ionization of the calorimeter material through which they pass. The similar ionization losses as well as nuclear interactions with the calorimeter material are experienced by charged pions. The separation parameter of $e^+e^- \rightarrow e^+e^-$ and $e^+e^- \rightarrow \pi^+\pi^-$ events with the energy $\sqrt{s} = 0.5 - 1.0$ GeV based on these differences has been developed.

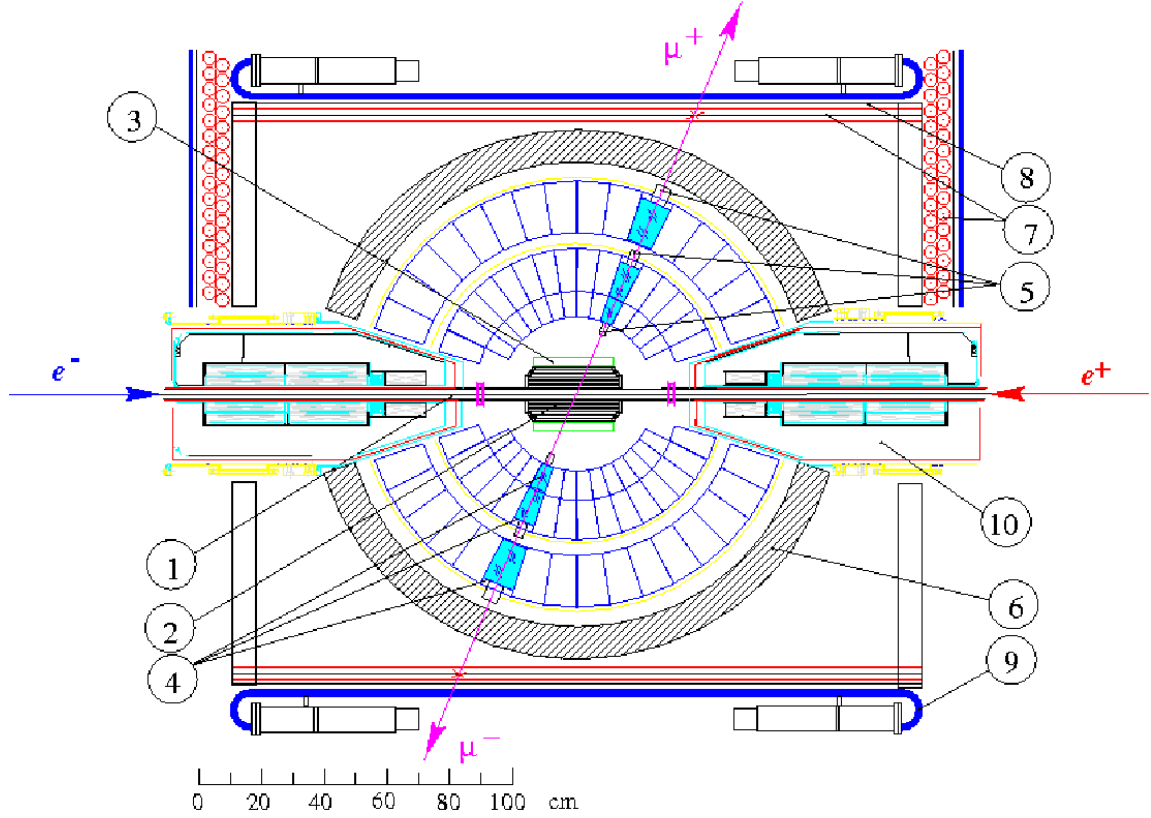


Figure 1. SND detector, section along the beams: (1) beam pipe, (2) tracking system, (3) aerogel Cherenkov counters, (4) NaI(Tl) crystals, (5) vacuum phototriodes (6) iron absorber, (7) proportional tubes, (8) iron plates, (9) scintillation counters, (10) solenoids of collider.

2. The SND calorimeter

SND detector [1] consists of the tracking system based on cylindrical drift and proportional chambers placed in a common gas volume, aerogel threshold counters [6], calorimeter and muon system based on proportional tubes and plastic scintillator. The solid angle of the tracking system is 94% of 4π and the resolutions in the azimuth and polar angles 0.45° and 0.8° , respectively. The threshold Cherenkov counters are based on aerogel with refractive index 1.05. The threshold momentums for $e/\mu/\pi$ are approximately equal to 1.6 / 330 / 436 MeV/c, respectively. The solid angle of the system is about 60% of 4π .

The main part of SND is three-layer spherical electromagnetic calorimeter based on NaI(Tl) crystals [1]. Pairs of counters of the two inner layers with thickness of 2.9 and 4.8 X_0 ($X_0 = 2.6$ cm) are sealed in thin (0.1 mm) aluminum containers, fixed to an aluminum supporting hemisphere (Fig. 2). Behind it, the third layer of NaI(Tl) crystals, 5.7 X_0 thick, is placed. The total calorimeter thickness for particles originating from the interaction region is 34.7 cm (13.4 X_0) of NaI(Tl). The total number of counters is 1632, the number of crystals per layer varies from 520 to 560. The angular dimensions of the most of crystals are $\Delta\phi = \Delta\theta = 9^\circ$, the total solid angle is 90% of 4π .

The scintillation light signals from the crystals are detected by vacuum phototriodes with an average photocathode quantum efficiency of about 15% and the mean tube gain of about 10. The

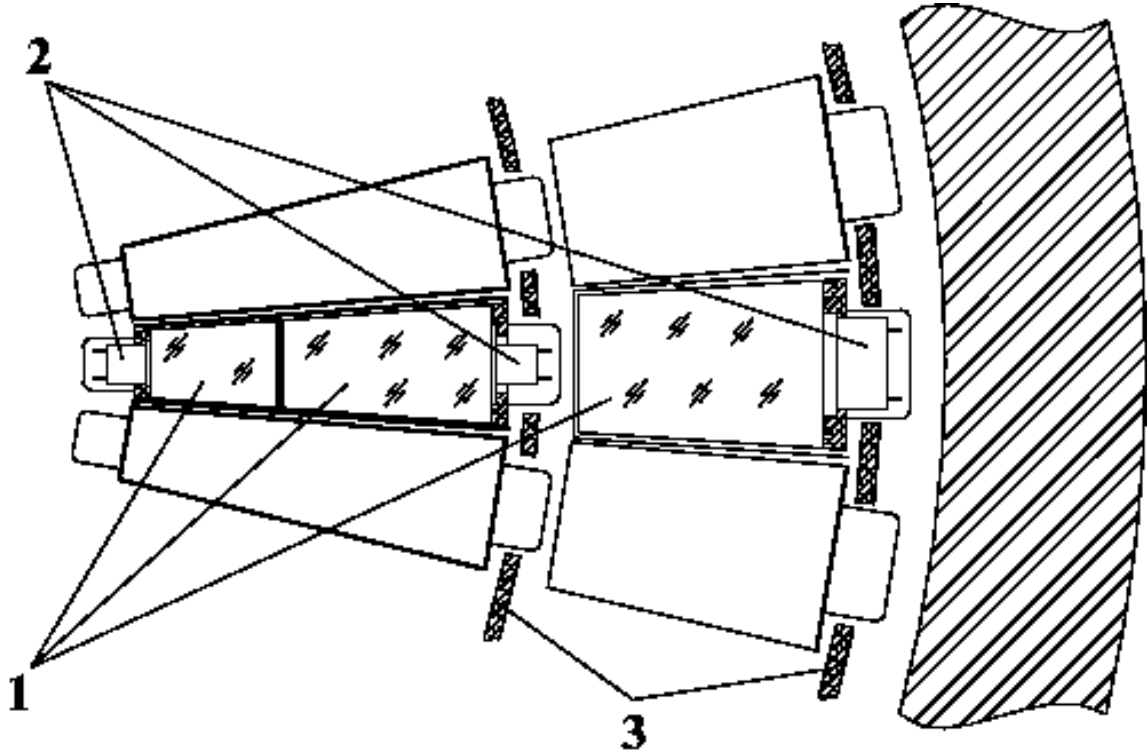


Figure 2. NaI(Tl) crystals layout inside the calorimeter: (1) NaI(Tl) crystals, (2) vacuum phototriodes, (3) aluminum supporting hemispheres.

electronics of the calorimeter consists of the charge sensitive preamplifiers with a conversion coefficient of 0.7 V/pC, shaping amplifiers and 12-bit analog to digital converter with a maximum input signal $U_{max} = 2$ V.

3. Separation parameter

The discrimination between electrons and pions in the SND calorimeter is based on the difference in the energy deposition profiles for these particles. The energy depositions in the layers of the calorimeter towers, that form the cluster related to the particle are used. Here the tower is the three counters of the 1, 2 and 3 layers with the same θ and ϕ coordinates. In particular the following parameters are used: 0E_j is the energy deposition in j th layer of the tower with the maximal energy deposition, 1E_j is the sum of energy depositions in j th layer of eight towers that surround the tower with the maximal energy deposition, 2E_j is the sum of energy depositions in j th layer of the other towers of the cluster ($j = 1, 2, 3$).

In order to use the correlations between energy depositions in the calorimeter layers in the most complete way, the corresponding separation parameter R was based on the machine learning approach. For each energy point the boosted decision trees network (forest) has been constructed [7]. The forest includes 900 trees, the maximal depth of a tree is 9. The 18 energy depositions kE_j and the average polar angle $\theta_0 = (\theta_1 - \theta_2 - 180^\circ)/2$ of the particles have been used as the discrimination variables. Here subscripts 1 and 2 denote the numbers of the particles. The training

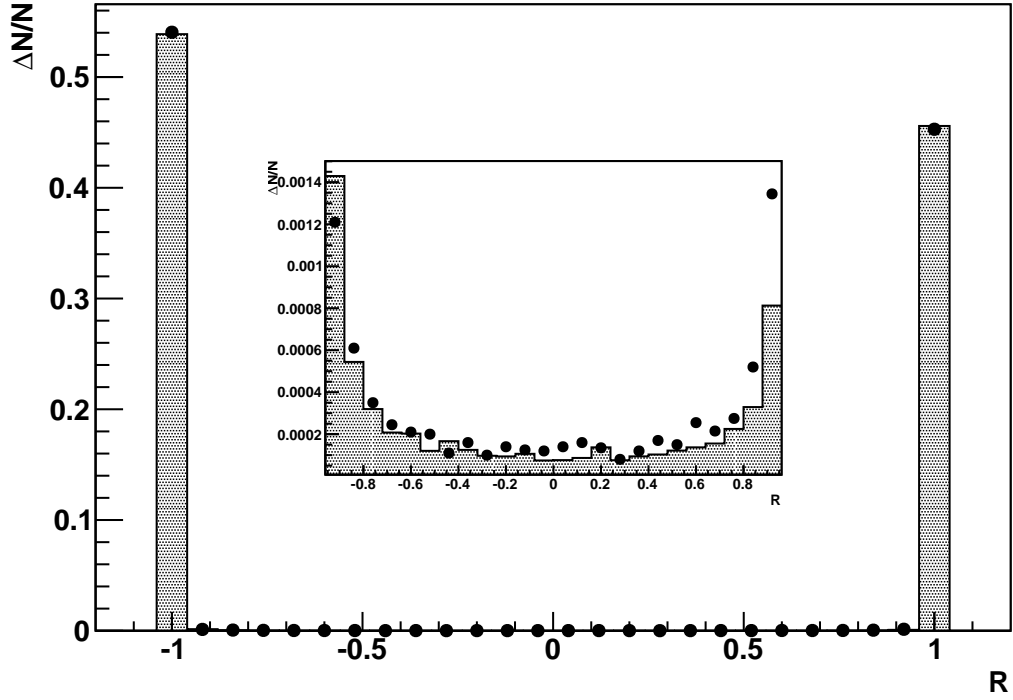


Figure 3. The e/π discrimination parameter R distribution for all collinear events at the energy $\sqrt{s} = 778$ MeV. Dots – experiment, histogram – simulation.

ensemble consists of simulated $e^+e^- \rightarrow \pi^+\pi^-$ and $e^+e^- \rightarrow e^+e^-$ events, that have passed the following cuts.

1. $N_{cha} = 2$. The events can contain neutral particles due to nuclear interactions of charged pions with detector material or due to electromagnetic showers splitting.
2. $|\Delta\theta| = |180^\circ - (\theta_1 + \theta_2)| < 8^\circ$ and $|\Delta\phi| = |180^\circ - |\phi_1 - \phi_2|| < 4^\circ$, where ϕ is the particle azimuthal angle.
3. $E_{1,2} > 40$ MeV, where E_i is the i th particle ($i = 1, 2$) energy deposition.
4. $50^\circ < \theta_0 < 130^\circ$.
5. The muon system $veto = 0$.

The output signal of the trained network (separation parameter) R is a value in the interval from -1.0 to 1.0 (Fig.3). The $e^+e^- \rightarrow e^+e^-$ events are located in the region $R < 0$, while $e^+e^- \rightarrow \pi^+\pi^-, \mu^+\mu^-$ events in $R > 0$.

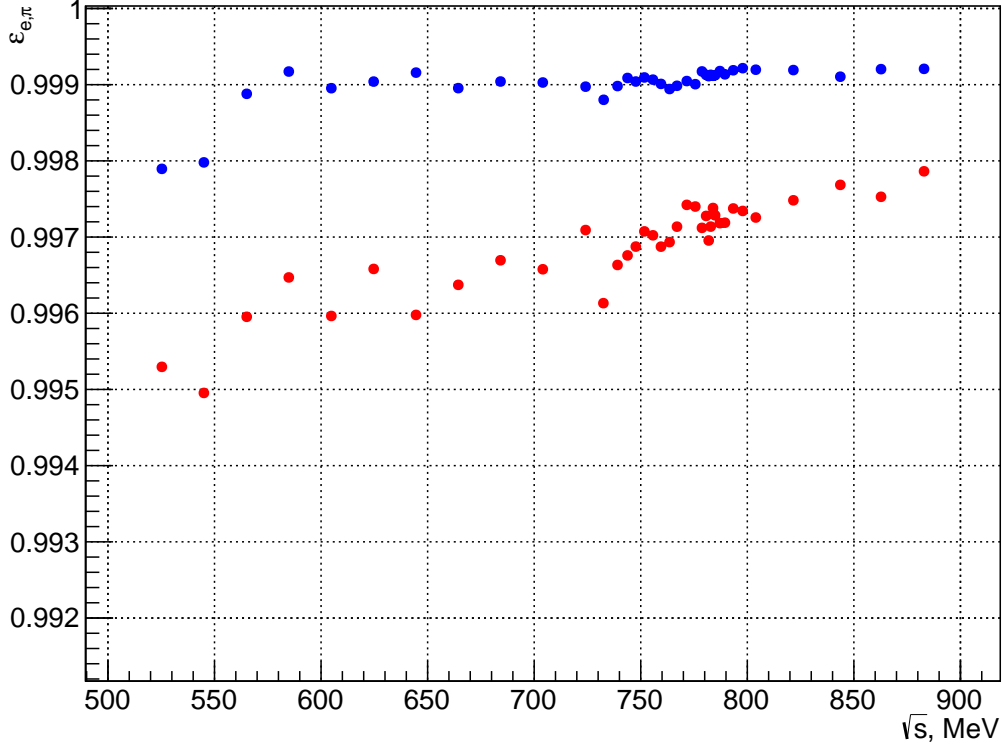


Figure 4. Identification efficiencies of $e^+e^- \rightarrow e^+e^-$ (red dots) and $e^+e^- \rightarrow \pi^+\pi^-$ (blue dots) events obtained using simulated events (the sample of 10^6 events of each process in each energy point was used). The statistical errors are less than the dots size.

4. Identification efficiency

Identification efficiencies

$$\varepsilon_e = \frac{N^{ee}(R \in [-1; 0])}{N^{ee}(R \in [-1; 1])}, \quad (4.1)$$

$$\varepsilon_\pi = \frac{N^{\pi\pi}(R \in [0; 1])}{N^{\pi\pi}(R \in [-1; 1])} \quad (4.2)$$

of the processes $e^+e^- \rightarrow e^+e^-$ and $\pi^+\pi^-$ obtained using simulated events are shown in Fig.4. Here $N^{ee,\pi\pi}(R \in [a; b])$ are the numbers of events of $e^+e^- \rightarrow e^+e^-$ and $\pi^+\pi^-$ processes in case if R belongs to the interval $[a; b]$. The efficiencies (Fig.4) exhibit not a statistical spread from point to point. This can be explained by the fact, that the number of the broken calorimeter channels are not coincident at different energy points.

Uncertainties in simulation of energy depositions in the calorimeter layers, in particular, simulation of pions nuclear interactions, leads to an inaccuracy in identification efficiencies. In order to estimate the systematic uncertainty of e/π discrimination, the pseudo- $\pi\pi$ and pseudo- ee events in the experiment and simulation have been formed in the following way.

The pseudo- ee event has been constructed from the particles of two separate collinear events demanding that their partners in these events look like electrons (have $R' < 0$ and aerogel counter has been fired by both charged particles). Analogously, pseudo- $\pi\pi$ event has been constructed using events in which the aerogel counter hasn't been fired and $R' > 0$. Here R' is e/π separation parameter based on the energy depositions ${}^k E_j$ of a single particle of the event. Identification efficiencies for simulated real and pseudoevents differs by 0.02% for e^+e^- and 0.01% for $\pi^+\pi^-$ events.

The experimental pseudo- $ee(\pi\pi)$ events contain small admixture of $\pi\pi(ee)$, $\mu\mu$, $e\pi$, $e\mu$, $\pi\mu$ events. Due to this background, identification efficiency for experimental pseudo- ee events is changed less than by 2×10^{-4} in the whole energy region $\sqrt{s} = 0.5 - 1.0$ GeV. In case of experimental pseudo- $\pi\pi$ events, efficiency is changing less than by 2×10^{-4} for the energy $\sqrt{s} > 0.6$ GeV, and below it changes up to 0.009 at the energy 0.5 GeV. The pseudo- $\pi\pi$ events with neglectable background contribution and higher statistics for the low energy region from 0.6 to 0.5 GeV have been constructed by using pions from the $e^+e^- \rightarrow \pi^+\pi^-\pi^0$ reaction. In order to construct the pseudo $\pi\pi$ event with the pions with the energy E_0 , two charged pions with energies E_π such that $|E_0 - E_\pi| < 5$ MeV have been used from two separate $e^+e^- \rightarrow \pi^+\pi^-\pi^0$ events. The $e^+e^- \rightarrow \pi^+\pi^-\pi^0$ events collected at the peaks of ω and ϕ mesons were used. The pions energies E_π have been obtained by using kinematic fit, which was performed under the following constraints: the charged particles are assumed to be pions, the system has zero total momentum, the total energy is \sqrt{s} , and the photons originate from the $\pi^0 \rightarrow \gamma\gamma$ decays. The difference between identification efficiencies of simulated $e^+e^- \rightarrow \pi^+\pi^-$ and simulated pseudo- $\pi\pi$ events of this type is 0.02%.

Using pseudoevents the correction coefficients for identification efficiencies of a real $e^+e^- \rightarrow e^+e^-$ and $e^+e^- \rightarrow \pi^+\pi^-$ events has been obtained as follows

$$\delta_x = \frac{\epsilon_x^{exp}}{\epsilon_x^{mc}}, \quad (4.3)$$

where $x = e(\pi)$, ϵ_x^{exp} and ϵ_x^{mc} are identification efficiencies for experimental and simulated pseudoevents respectively. The energy dependencies of the correction coefficients are shown in Fig.5. The δ_e coefficient does not depend on energy, its average value is equal to 1.0006 ± 0.0001 . The values of correction coefficients δ_π obtained using pseudo $\pi\pi$ events constructed from $e^+e^- \rightarrow \pi^+\pi^-$ and $e^+e^- \rightarrow \omega, \phi \rightarrow \pi^+\pi^-\pi^0$ events are in agreement within their statistical errors. Their energy dependence was fitted by the function

$$\delta_\pi(\sqrt{s}) = a \left(\sqrt{(\sqrt{s} - b)^2 - 10(\sqrt{s} - b)} - (\sqrt{s} - b) \right) + c. \quad (4.4)$$

It was obtained that $\delta_\pi = 0.9990 \pm 0.0002$ at the energy region \sqrt{s} above 0.65 GeV and below δ_π changes upto 0.9950 ± 0.0006 at $\sqrt{s} = 0.52$ GeV (Fig.5).

The total error of the correction coefficient determination is

$$\sigma_{tot} = \sigma_{stat} \oplus \sigma_{ID} \oplus \sigma_{bkg}. \quad (4.5)$$

Here σ_{stat} is the statistical error, σ_{ID} is the difference in identification efficiency for real and pseudoevents, σ_{bkg} is the change of identification efficiency for experimental pseudoevents due to background admixture. The magnitudes for various contributions to the total error are shown in table 1.

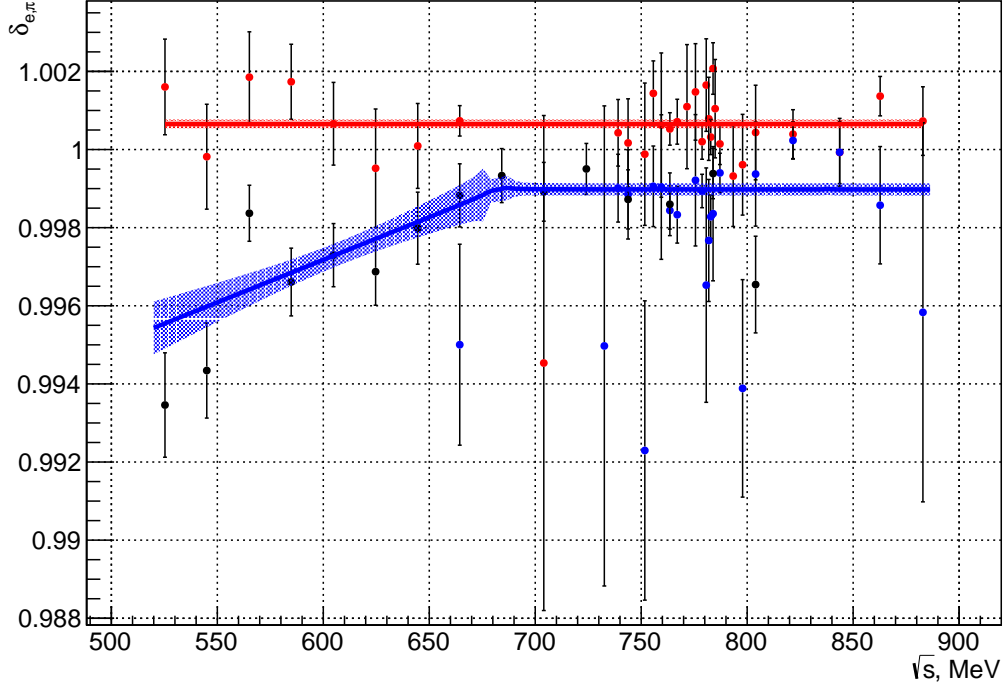


Figure 5. Correction coefficients for identification efficiencies of $e^+e^- \rightarrow e^+e^-$ (red dots) and $e^+e^- \rightarrow \pi^+\pi^-$ (blue and black dots) events. The blue and black dots show the values of δ_π obtained using pseudo $\pi\pi$ events constructed from $e^+e^- \rightarrow \pi^+\pi^-$ and $e^+e^- \rightarrow \omega, \phi \rightarrow \pi^+\pi^-\pi^0$ events, respectively. Lines are the results of approximations, dashed regions show the errors.

Table 1. Various contributions to the relative errors of the δ_e and δ_π correction coefficients.

Error	Contribution to δ_e , %	Contribution to δ_π at $\sqrt{s} > 0.65$ GeV, %	Contribution to δ_π at $\sqrt{s} < 0.65$ GeV, %
σ_{stat}	0.01	0.02	0.02 – 0.06
σ_{ID}	0.02	0.01	0.02
σ_{bkg}	0.02	0.02	–
σ_{tot}	0.03	0.03	0.03 – 0.06

The total relative error of δ_e is $\sigma_{tot} = 0.03\%$ and of δ_π is $\sigma_{tot} = 0.03\%$ at $\sqrt{s} > 0.65$ GeV and $\sigma_{tot} = 0.03 - 0.06\%$ at $\sqrt{s} < 0.65$ GeV.

The corrected identification efficiencies of processes $e^+e^- \rightarrow e^+e^-$ and $e^+e^- \rightarrow \pi^+\pi^-$ are shown in Fig.6. Their errors are dominated by the errors of the correction coefficients. Contribution of the identification efficiencies errors to the total relative error of $e^+e^- \rightarrow \pi^+\pi^-$ cross section (1.1) is shown in Fig.7 and is less than 0.2% for the most energy points.

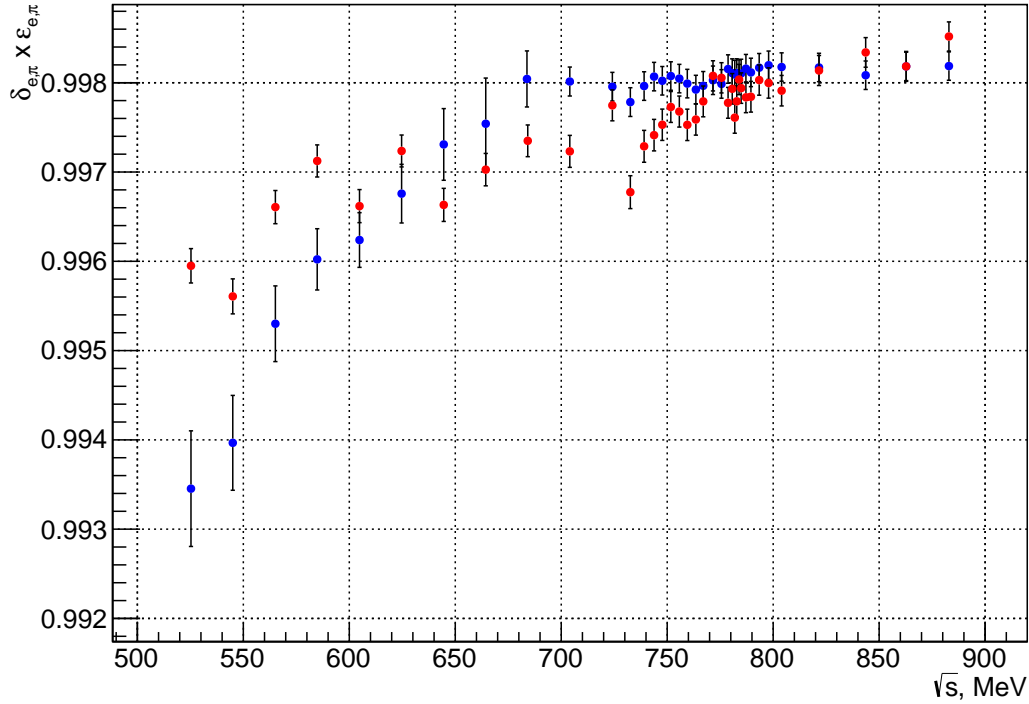


Figure 6. Corrected identification efficiencies $\delta_e \epsilon_e$ and $\delta_\pi \epsilon_\pi$ of $e^+e^- \rightarrow e^+e^-$ (red dots) and $e^+e^- \rightarrow \pi^+\pi^-$ (blue dots) events.

5. Conclusion

The technique of discrimination of the $e^+e^- \rightarrow e^+e^-$ and $e^+e^- \rightarrow \pi^+\pi^-$ events using energy deposition in the calorimeter of SND detector has been developed. Identification efficiency for $e^+e^- \rightarrow e^+e^-$ and $e^+e^- \rightarrow \pi^+\pi^-$ events has been obtained. Contribution of the identification efficiencies errors to the total error of $e^+e^- \rightarrow \pi^+\pi^-$ cross section is less than 0.2% for the most energy points.

Acknowledgments

This work was supported in part by the RFBR grants 14-02-00129-a and 16-32-00542-mol-a, part of this work related to reconstruction of clusters in calorimeter was supported by Russian Science Foundation (project N 14-50-00080).

References

- [1] M.N.Achasov et al., *Spherical neutral detector for VEPP-2M collider*, *Nucl. Instr. Meth.* **A 449** (2000) 125
M.N. Achasov, et. al., *Spherical Neutral Detector for experiments at VEPP-2000 e^+e^- collider*, in proceedings of *International Workshop on ee collisions from Phi to Psi*, September 19 – 22, 2011 Novosibirsk, Russia, *Nucl. Phys. Proc. Suppl.* **225-227** (2012) 66

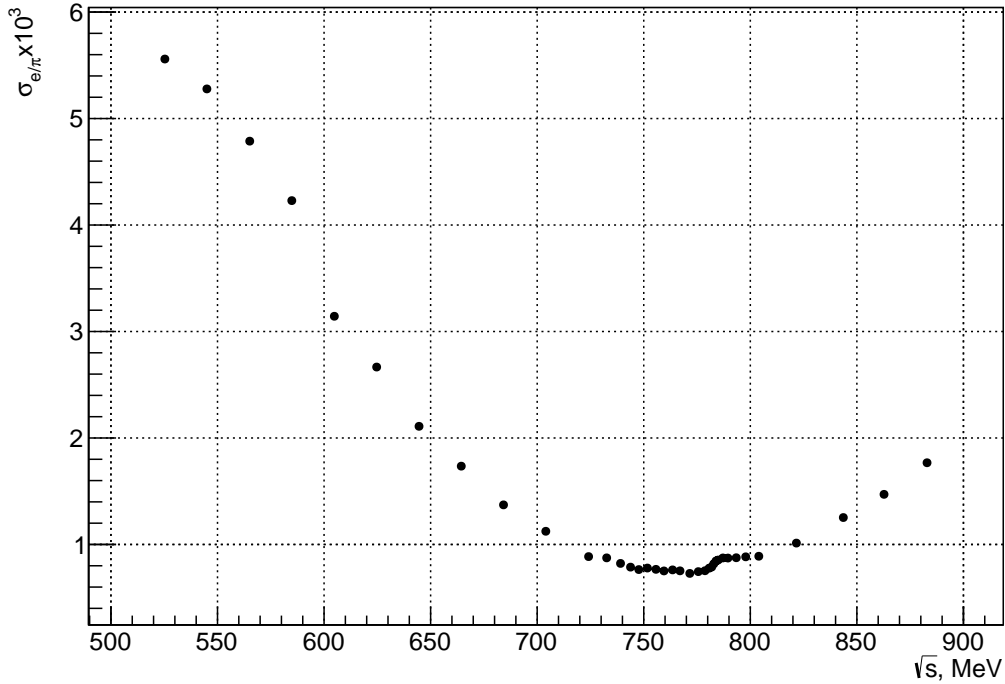


Figure 7. The relative error $\sigma_{e/\pi}$ of $e^+e^- \rightarrow \pi^+\pi^-$ cross section due to the errors of identification efficiencies at the different energy points.

- [2] D.E. Berkaev et al., *Electron-positron collider VEPP-2000. First experiments*, *Zh. Eksp. Teor. Fiz.* **140** (2011) 247;
 E.V. Abakumova et al., *A system of beam energy measurement based on the Compton backscattered laser photons for the VEPP-2000 electron-positron collider*, *Nucl. Instr. Meth. A* **755** (2014) 35;
 E.V. Abakumova et al., *The system for delivery of IR laser radiator into high vacuum*, *JINST* **10** (2015) T09001.
- [3] I. Logashenko, et. al., *The Measurement of the Anomalous Magnetic Moment of the Muon at Fermilab*, *J. Phys. Chem. Ref. Data* **44** (2015) 031211
- [4] I.B. Logashenko, et al., *Measurement of the hadronic cross sections at Novosibirsk*, in proceedings of *International Conference Dark Matter, Hadron Physics and Fusion Physics*, September 24 – 26, 2014 Messina, Italy, *EPJ Web Conf.* **96** (2015) 01022
- [5] R. R. Akhmetshin, et. al., *Measurement of $e^+e^- \rightarrow \pi^+\pi^-$ cross-section with CMD-2 around ρ -meson*, *Phys. Lett.* **B 527** (2002) 161;
 M. N. Achasov, et. al., *Study of the process $e^+e^- \rightarrow \pi^+\pi^-$ in the energy region $400 < \sqrt{s} < 1000$ MeV*, *Zh. Eksp. Teor. Fiz.* **128** (2005) 1201 [*J. Exp. Theor. Phys.* **101** (2005) 1053];
 R. R. Akhmetshin, et. al., *High-statistics measurement of the pion form factor in the ρ -meson energy range with the CMD-2 detector*, *Phys. Lett.* **B 527** (2007) 28.
- [6] A.Yu. Barnyakov, et. al., *Testing aerogel Cherenkov counters with $n = 1.05$ using electrons and muons*, *Prib. Tekh. Eksp.* **1** (2015) 37 [*Instrum. Exp. Tech.* **58** (2015) 30]

- [7] A. Hoecker, et.al., *TMVA - Toolkit for Multivariate Data Analysis*, in proceedings of *11th International Workshop on Advanced Computing and Analysis Techniques in Physics Research*, April 23 – 27, 2007 Amsterdam, The Netherlands, *PoS ACAT2007* (2007) 040 [physics/0703039].